

Kerstin Tittes · Andreas Bund · Waldfried Plieth  
Anders Bentien · Silke Paschen · Matthias Plötner  
Hartmut Gräfe · Wolf-Joachim Fischer

## Electrochemical deposition of Bi<sub>2</sub>Te<sub>3</sub> for thermoelectric microdevices

Received: 28 November 2002 / Accepted: 6 March 2003 / Published online: 21 May 2003  
© Springer-Verlag 2003

**Abstract** The electrolyses of solutions of bismuth oxide and tellurium oxide in nitric acid with molar ratios of Bi:Te = 3:3–4:3 lead to cathodic deposits of films of bismuth telluride (Bi<sub>2</sub>Te<sub>3</sub>), an n-type semiconductor. Current densities of 2–5 mA/cm<sup>2</sup> were applied. Voltammetric investigations showed that Bi<sub>2</sub>Te<sub>3</sub> deposition occurred at potentials more negative than –0.125 V (Ag/AgCl, 3 M KCl). The deposit was identified as bismuth telluride ( $\gamma$ -phase) by X-ray analysis. Hall-effect measurements verified the n-type semiconducting behaviour. The films can be deposited in microstructures for thermoelectric microdevices like thermoelectric batteries or thermoelectric sensors.

**Keywords** Bismuth telluride films · Cyclic voltammetry · Electrodeposition · Thermoelectric battery · Thermoelectric sensor

### Introduction

A good thermoelectric material should have large thermoelectric power (Seebeck coefficient,  $\alpha$ ) to produce the required voltage, low thermal conductivity ( $\lambda$ ) to keep the heat at the junction and low electrical resistivity ( $\rho$ ) to minimize Joule heating. Bismuth telluride, bismuth antimony telluride and bismuth selenium telluride are promising candidates for thermoelectric

devices (Table 1) [1]. The compounds have markedly higher Seebeck coefficients and thermoelectric figures of merit [ $\alpha^2/(\rho^*\lambda)$ ] than the elements antimony and bismuth. Thus p- and n-bismuth tellurides have been used as so-called leg materials in thermobatteries. The films were deposited by evaporation techniques, like other thermoelectric materials. Because of the specific application, modified requirements for the energy supply for self-supporting microsystems are needed, and various criteria for the optimization of the materials, the design and the technology arise, compared to commonly known concepts for thermoelectric generators. While thin film technology or assembly of crystal elements are employed for the fabrication of sensors or thermoelectric coolers, electrodeposition may be at the focus for microsystem applications. Because the output voltages are still low, chaining of several couples to a single device and several chains to a battery are necessary. The single batteries may be stacked to give larger generators, employing mechanical drilling and conducting adhesive bonding between the stacks [2]. Bismuth telluride in both the p- and n-type semiconducting forms has been chosen as a material in these thermobatteries, due to its good thermoelectric properties. Galvanic deposition of this material would be a striking low-cost version for building up the required structures.

In the phase diagram [3], the Bi<sub>2</sub>Te<sub>3</sub> phase exists in a region of 59.5–60.5 atom% Te. In the literature [4], phase widths of 59.0–62.6 at% Te for p-type semiconducting and 62.6–66.0 at% for n-type semiconducting for Bi<sub>2</sub>Te<sub>3</sub> are reported. This method using electrochemical deposition for manufacturing such electronic grade materials for thick film electronic microdevices looks very promising.

The investigations described in this paper are based on the work of Magri et al. [5, 6] and Fleurial et al. [7]. These authors deposited bismuth-tellurium compounds from nitric acid electrolytes with different compositions, and studied the systems with voltammetry and X-ray analysis.

K. Tittes · A. Bund · W. Plieth (✉)  
Institute of Physical Chemistry and Electrochemistry,  
Technische Universität Dresden, 01062 Dresden, Germany  
E-mail: waldfried.plieth@chemie.tu-dresden.de

A. Bentien · S. Paschen  
Max Planck Institute for Chemical Physics of Solids,  
Nöthnitzer Strasse 40, 01187 Dresden, Germany

M. Plötner · H. Gräfe · W.-J. Fischer  
Semiconductor Technology and Microsystems Laboratory,  
Technische Universität Dresden, 01062 Dresden, Germany

**Table 1** Properties of selected thermoelectric materials at room temperature [1]

Element/compound	$\alpha$ ( $10^{-6}$ V K $^{-1}$ )	$\alpha^2/(\rho^*\lambda)$ ( $10^{-3}$ K $^{-1}$ )
(Bi $_{2-x}$ Sb $_x$ )Te $_3$	210	1–3
p-Bi $_2$ Te $_3$	140	
p-Si	1300	0.0001
Sb	48	0.03
NiCr (80/20)	25	0.04
Cr	22	0.03
Ni	-20	0.04
Cu/Ni	-35	0.09
Bi	-68	0.3
n-Bi $_2$ Te $_3$	-110 to -250	1–3
Bi $_2$ (Se $_x$ Te $_{3-x}$ )	-250	

**Fig. 1** Cyclic voltammograms of the separately investigated components of the deposition electrolyte: 10 mM Bi, 1 M HNO $_3$  (solid line); 12 mM Te, 1 M HNO $_3$  (dotted line).  $T=298$  K; Pt working electrode; scan rate 0.01 V/s

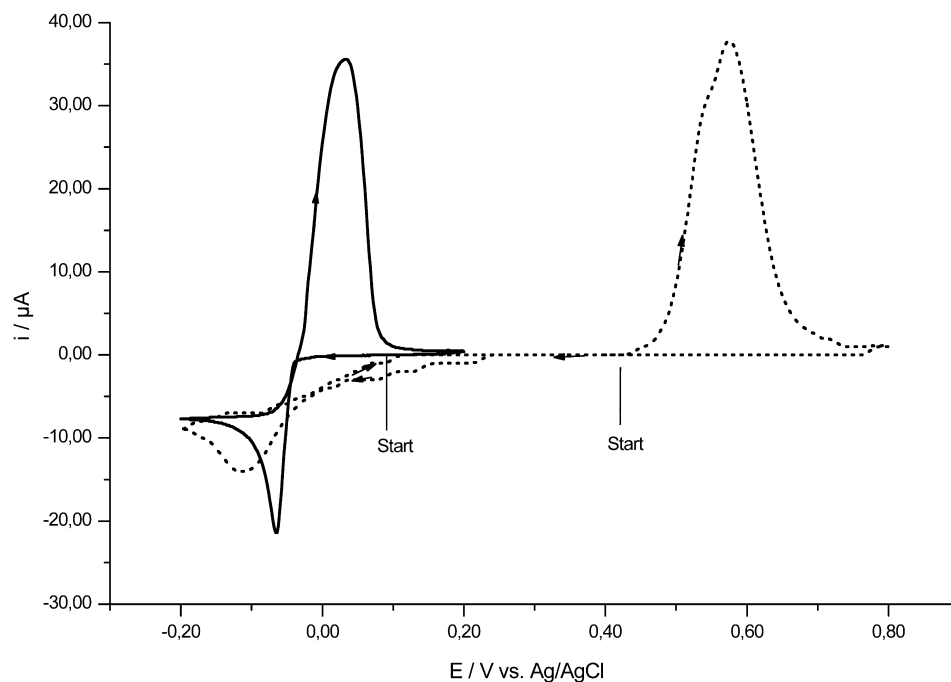


**Fig. 2** Sampling experiments at the potentials of the preferred tellurium deposition. Sampling (30 s) proceeds during the 1st scan; Pt working electrode; scan rate 0.05 V/s; 12.6 mM Bi, 6.3 mM Te, 1 M HNO $_3$

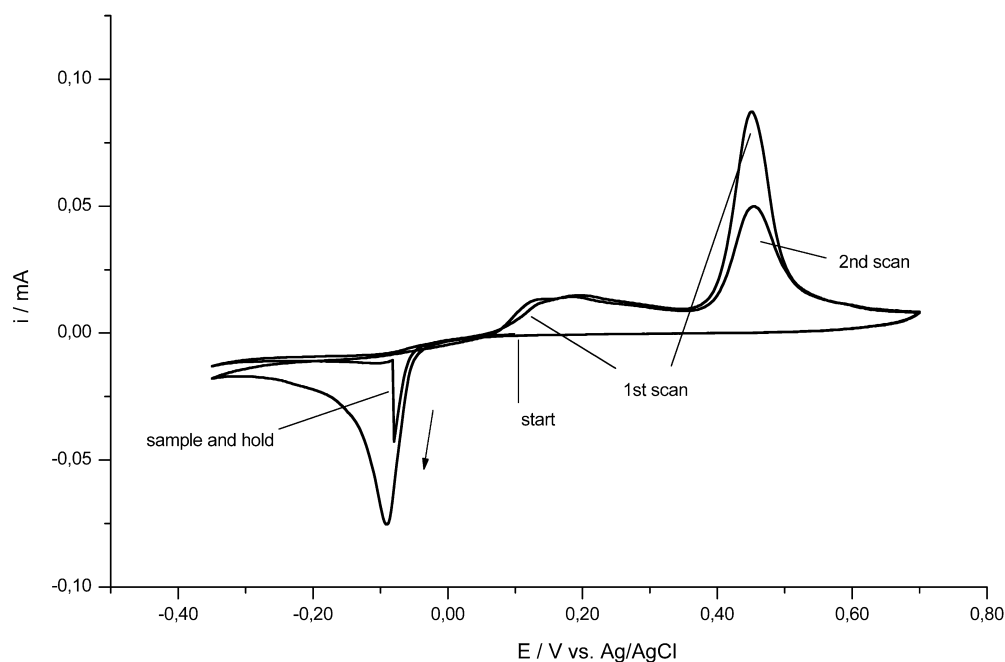


**Fig. 3** Sampling experiment in the limiting current of the Bi deposition process. Bi-Te electrolyte: 12.6 mM Bi, 6.3 mM Te, 1 M HNO<sub>3</sub>; Pt working electrode; scan rate 0.05 V/s; sampling (30 s) proceeds during the 1st scan

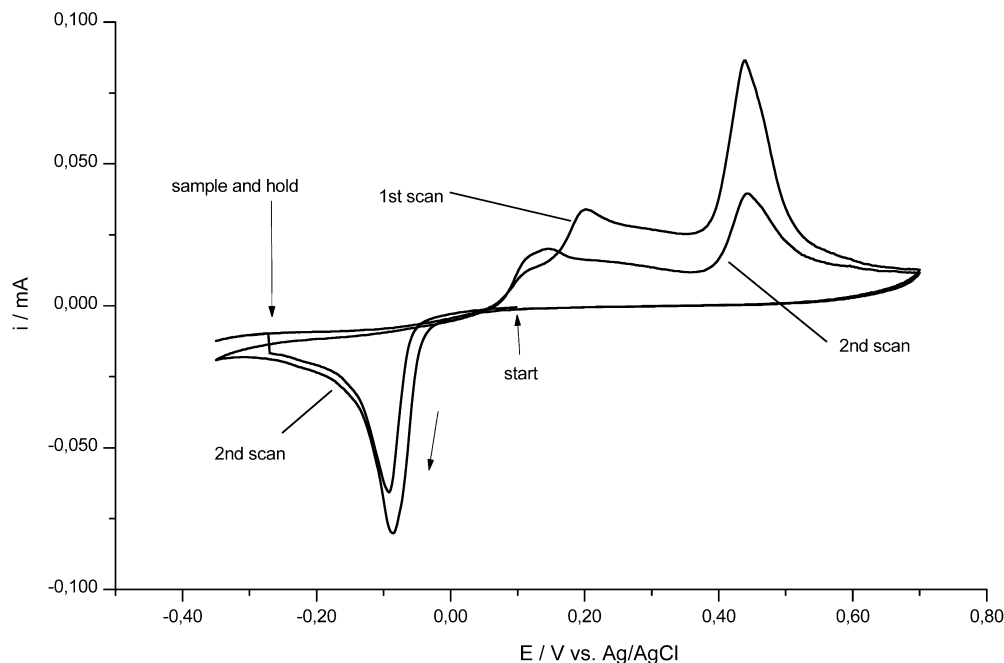
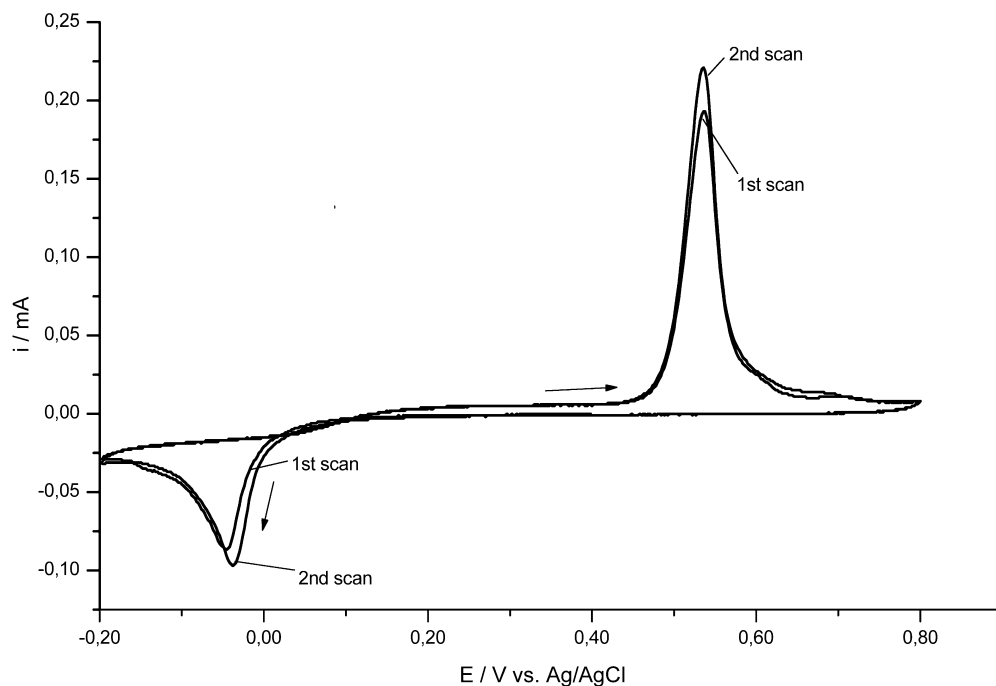


**Fig. 4** Cyclic voltammogram of the deposition/stripping process for bismuth telluride from an optimized electrolyte: 8.2 mM Bi, 10.3 mM Te, 1 M HNO<sub>3</sub>; Pt working electrode; scan rate 0.1 V/s



## Experimental

The electrolyte was made by dissolution of bismuth oxide (99.8%; Chempur) and tellurium(IV) oxide (99.99%; Alfa Aesar) in nitric acid (1 mol/L; Baker, p.a. grade), following the best results for Te anode dissolution. The concentration of the components was  $5 \times 10^{-3}$  M to  $12.5 \times 10^{-3}$  M tellurium, which exist as telluryl ions ( $\text{HTeO}_2^+$ ) [8, 9], and  $5 \times 10^{-3}$  M to  $12.6 \times 10^{-3}$  M bismuth ( $\text{Bi}^{3+}$ ). The bismuth/tellurium concentration ratio was varied between 4:3 and 3:4. The pH value of the electrolyte was 0.4.

Copper and nickel foils with a thickness of 50–70  $\mu\text{m}$  were used as substrates for the working electrodes. The nickel foils

were degreased by dichloromethane vapor, etched 2 min in concentrated HCl, rinsed with distilled water, treated with ethanol and subsequently dried. Platinated titanium stretch metal or bismuth/tellurium alloy were used as counter electrodes. The coated substrate was rinsed after electrolyses with 0.1 M nitric acid (pH 1), distilled water and ethanol. Then the samples were dried in air and analysed.

The alloy depositions occurred galvanostatically. Current densities in the range of 1–10  $\text{mA}/\text{cm}^2$  were applied. The electrolyses were carried out under isothermal conditions (298 K) in a stirred solution (magnetic stirrer: 500–1250 rpm). A 263A potentiostat (EG&G) and a Statron 3208 direct current source (VEB Statron Fürstenwalde) were used for the experiments.

**Fig. 5** Dependence of the deposition/stripping process on the temperature: cyclic voltammograms on rotating disk electrodes; working electrode: rotating Pt disc,  $d=0.35$  cm,  $v_{\text{rot}}=300$  rpm; scan rate 0.01 V/s; counter electrode: Pt sheet; reference: SCE; 8.2 mM Bi, 10.3 mM Te, 1 M HNO<sub>3</sub>

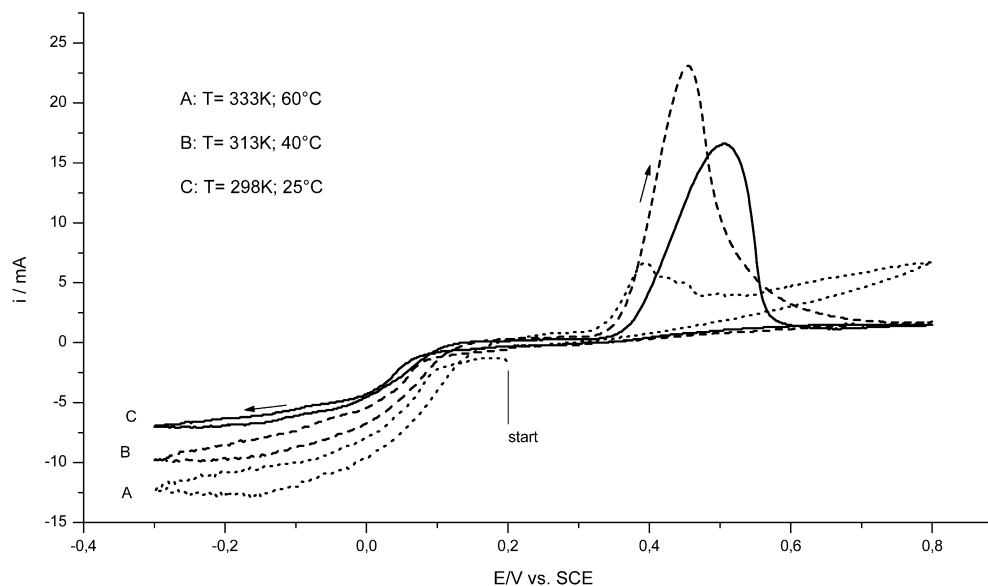
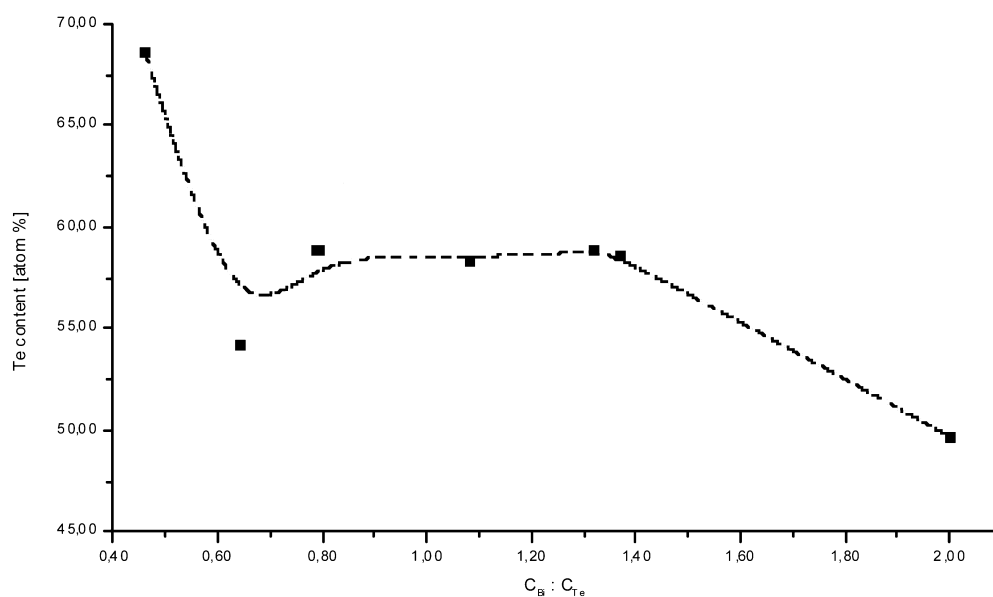


**Fig. 6** The dependence of the tellurium content of the alloy deposit on the concentration ratio of Bi:Te in the bulk electrolyte at a constant current density (5 mA/cm<sup>2</sup>) and under constant stirring (500 rpm)



The bismuth concentration was determined by complexometric back-titration with 1,2-diaminocyclohexanetraacetic acid (Titrplex IV; Merck) with zinc sulfate against xylenol orange (Idranal, Riedel de Haen-Firmenschrift). The tellurium(IV) concentration was determined potentiometrically by redox titration of the chromium(VI) excess with Fe(II) ions [10, 11].

The surface morphology of the deposited alloys was studied by scanning electron microscopy (DSM 982, Zeiss Oberkochen). The bismuth and tellurium content of the deposits was investigated with the help of EDX microanalyses. For the quantitative analysis the EDX analyser was calibrated by a bismuth telluride standard (99.999 mass% Bi<sub>2</sub>Te<sub>3</sub>; Alfa Aesar). The standard was measured at 5 points, each with 4000 counts. The values were accumulated and set as 40 at% bismuth and 60 at% tellurium. A subsequent comparative test analysis of the standard showed a tellurium content of 59.95 at%.

For the investigation of the averaged bismuth and tellurium content, the deposited alloy layers were analysed at 5 points. The lateral distribution could be estimated by line scans and mapping.

For comparable measurements, ICP-OES (inductive coupled plasma-optical emission spectroscopy) was used. The analyses were performed according to DIN EN ISO 11855. The deep profile analyses by glow-discharge OES yielded the qualitative composition of the layers.

Phase identification of the layers was carried out by X-ray diffractometry (Siemens D5000; Cu K<sub>α</sub> radiation)

The voltammetric investigations were carried out with 263A and 273A potentiostats (EG&G). A platinum wire was used as counter electrode in 0.1 M HNO<sub>3</sub>. The reference system was a 3 M Ag/AgCl electrode. The counter and the reference electrodes were separated from the sample electrolyte by so-called "Vycor tips", a porous glass diffusion barrier. Metal wires (Pt, Cu, Ni, Ag), glass sealed and plain polished at the front side with an area of 0.5–0.8 mm<sup>2</sup>, acted as the working electrodes. For fabrication of the tellurium electrodes the analysis grade substance (99.999 mass%; Fa. ABCR) was sealed in a glass tube by epoxy resin and electrically contacted by silver epoxy. Bismuth telluride and bismuth were sealed/moulded in glass tubes and contacted with copper wires. The pretreatment or regeneration was done by polishing in combination

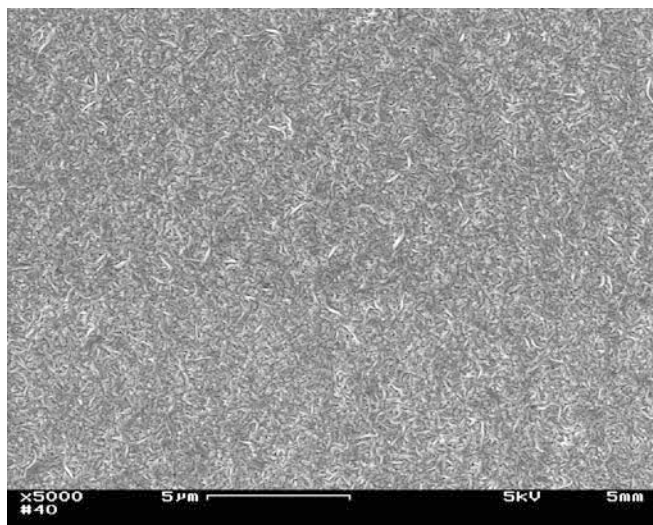


**Fig. 7** SEM micrograph of a Bi-Te layer (enlarged 5000 $\times$ ). Composition: 41.1 at% Bi, 58.9 at% Te; thickness of the layer: 9  $\mu\text{m}$ ; electrolyte: 10.8 mM bismuth, 8.2 mM tellurium, 1 M  $\text{HNO}_3$ ; conditions: 5  $\text{mA}/\text{cm}^2$ , 500 rpm

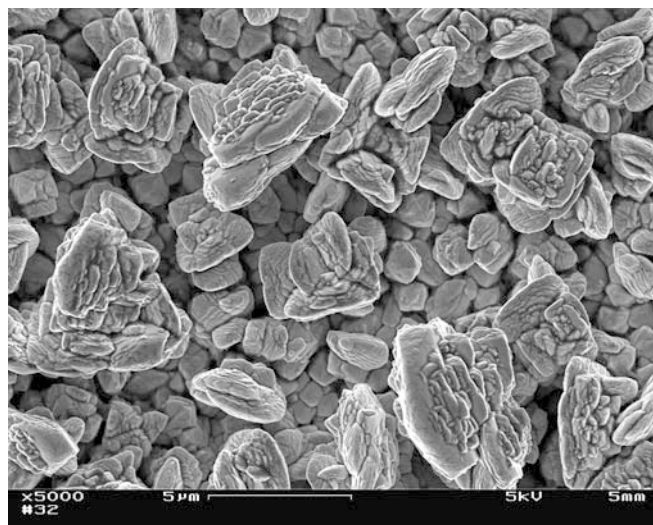
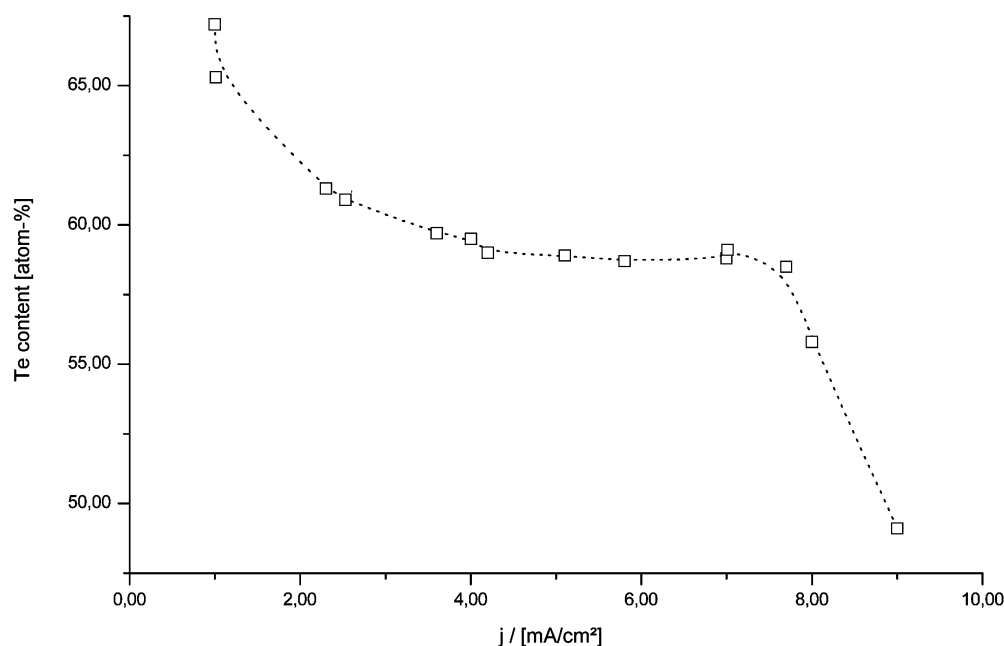


**Fig. 8** SEM micrograph of a Bi-Te layer (enlarged 5000 $\times$ ). Composition: 31.3 at% Bi, 68.7 at% Te; electrolyte: 5.7 mM bismuth, 12.4 mM tellurium, 1 M  $\text{HNO}_3$ ; conditions: 5  $\text{mA}/\text{cm}^2$ , 500 rpm

with rinsing in dilute  $\text{HNO}_3$  and twice with distilled water. A micro-cell (EG&G;  $V=3\text{ mL}$ ) was used in most of the voltammetric investigations.

Hall-effect measurements were performed on film pieces with typical dimensions of  $1\times 1\text{ mm}^2$  and thickness from 6 to 20  $\mu\text{m}$ . The pieces were peeled off mechanically from the substrates. Before the contacts were mounted with silver paste, the samples were left in weak  $\text{HCl}$  for several hours in order to remove any leftovers from the substrate. All Hall-effect measurements were performed at 300 K. The magnetic field was approximately perpendicular to the film plane and an a.c. current was applied to the film. The Hall voltage contacts were close to perpendicular to the direction of the current. In order to eliminate the (small) misalignment, the samples were, at each temperature and field setting, first measured in an upright position with respect to the field, then turned by  $180^\circ$  and measured again. The Hall voltage was obtained as the asymmetric contribution under sample reversal.

**Fig. 9** The dependence of the tellurium content of the layer on the current density within a constant tellurium bulk concentration. Electrolyte composition: 10.8 mM Bi, 8.2 mM Te, 1 M  $\text{HNO}_3$ . Stirring velocity: 500 rpm



## Results

In the first experiments, copper foils were used as substrates. The layers showed a crystalline structure and a tarnished surface. At the beginning of the electrocrystallization process the electrodeposition of tellurium occurred. The formation of bismuth-rich compounds occurred not before the molar ratio of Bi:Te in the solution became greater than 2:1. During the deposition under strong convection conditions, mechanical tensions occurred in the layers, causing a partial peeling of the deposits. If the alloys were deposited on a copper substrate, the deposits contained traces of the substrate.

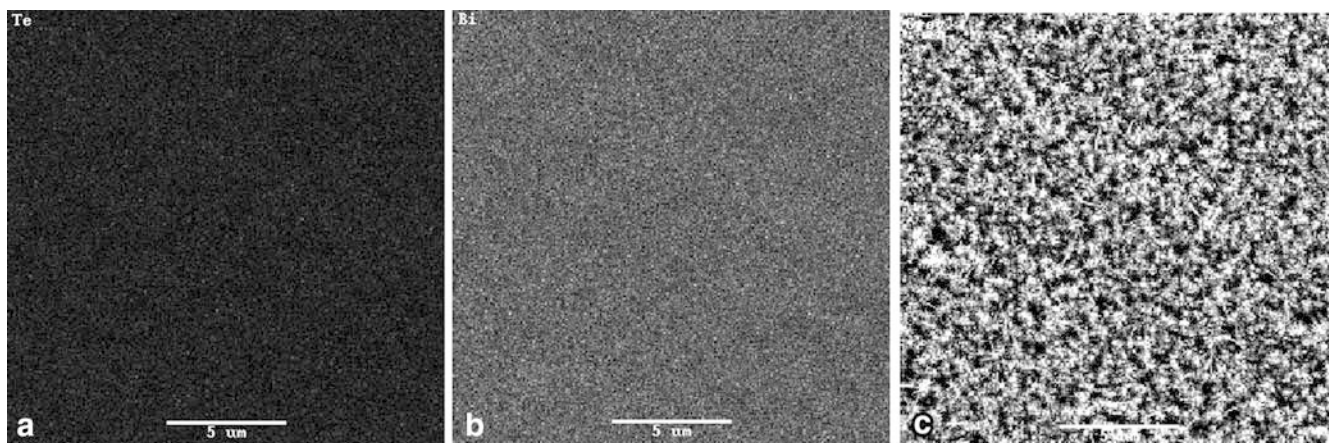


**Fig. 10** EDX mapping of the bismuth-tellurium surface: (a) Te reflexes; (b) Bi reflexes; (c) SEM micrograph. Area:  $18 \times 18 \mu\text{m}^2$ ; enlarged 5000 $\times$ ; composition: 41.2 at% Bi, 58.8 at% Te; thickness of the layer: 10  $\mu\text{m}$

Copper contamination has a dramatic influence on the electronic properties of the bismuth tellurides [12]: it transforms p-type semiconducting bismuth telluride into an n-type semiconducting material. Therefore copper could not be used as a substrate. Either the copper foils were galvanized by Ni, or Ni foils had to be used. On the Ni substrates the deposition conditions were systematically investigated.

Cyclic voltammetry was used to determine the electrochemical characteristics of the components (Fig. 1). The tellurium deposition started at a potential of +0.23 V vs. Ag/AgCl. The shape of the corresponding curve of the unstirred solution could be interpreted as a reduction/deposition of different tellurium layer structures on the substrate or the additional occurrence of adsorption pre-peaks [8, 14]. The anodic oxidation/stripping process of tellurium did not take place before +0.4 V. The dissolution/deposition process of Bi was reversible, neglecting a small crystallization overpotential. The voltammograms showed a cathodic peak–half-peak difference,  $|E_P - E_{P/2}|$ , of 18.5 mV according to the 19 mV diagnostic criterion of a solid electrode product [15, 16]. The deposition began at  $-0.03$  V and a maximum occurred at  $-0.07$  V; in the reverse scan the maximum of the oxidation peak occurred at +0.06 V. Because of the more positive potential at the start of the Te deposition, one had to expect that prior to Bi deposition the working electrode was coated with Te and only after passing the Bi deposition potential did the alloy coating start. An electrolyte that contained bismuth and tellurium showed a quite different voltammogram. A single deposition peak at  $-0.09$  V was found and no typical anodic Bi-stripping peak was observed. The beginning of the oxidation was shifted to +0.1 V, with a broad maximum at +0.48 V. Accumulation experiments should help to identify the corresponding dissolution peaks of the deposited species. If the potential was kept constant over a definite time (30 s) in the region of the favoured tellurium deposition

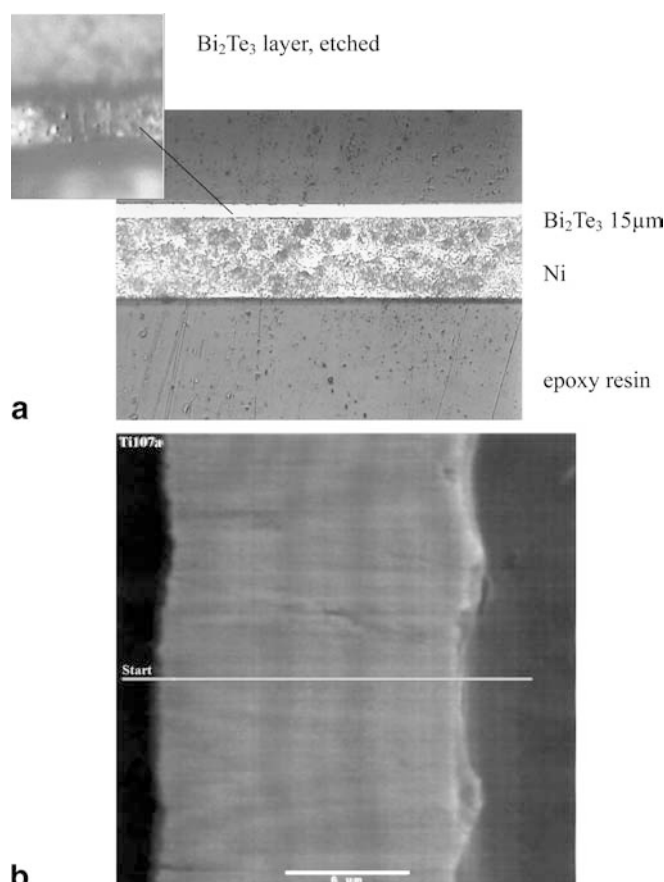
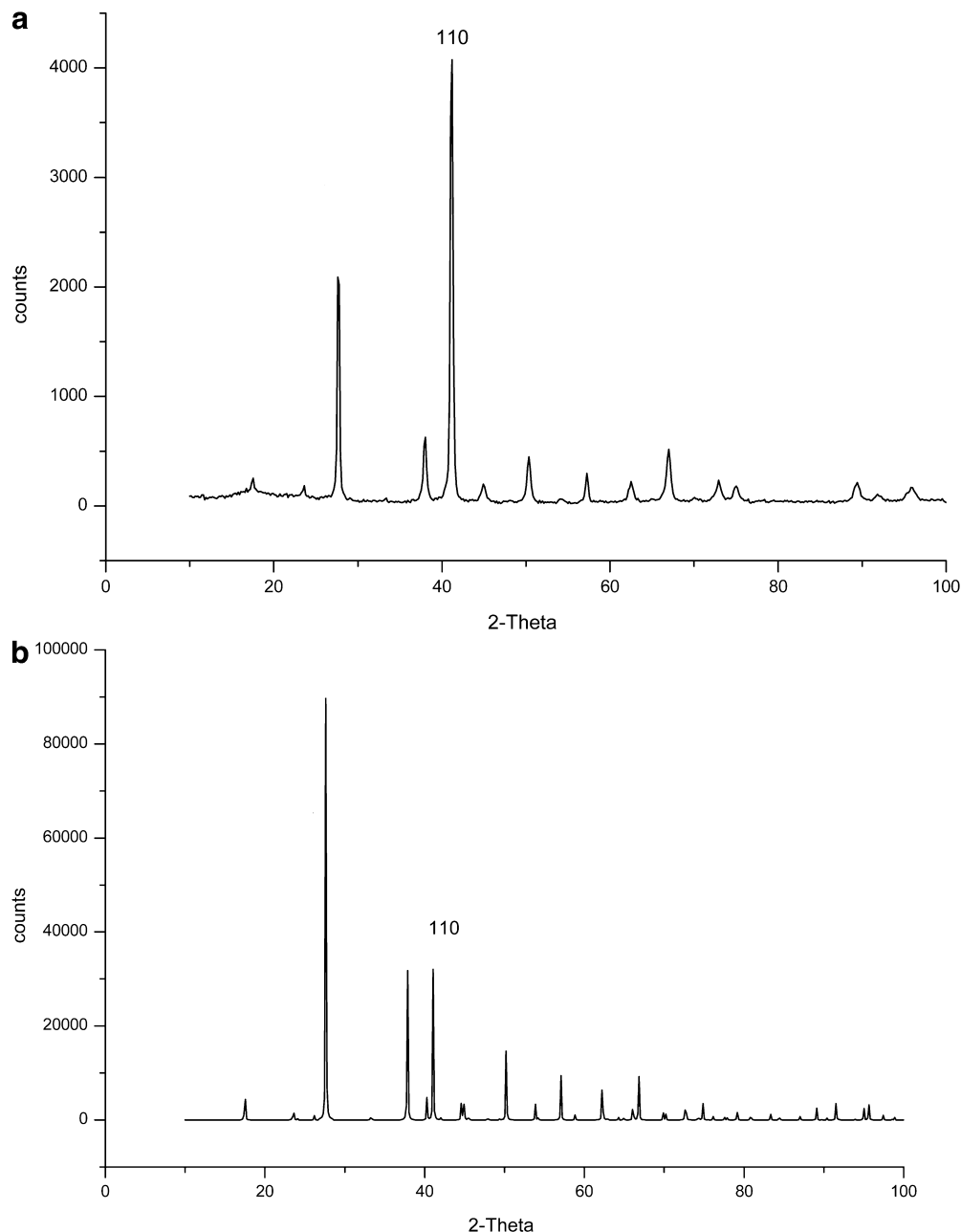


**Fig. 11** Micrograph analysis of an etched bismuth telluride deposit: (a) micrograph of the cross-section of bismuth-telluride deposit on nickel substrate; (b) SEM micrograph/EDX investigations. Surface: 41.5 at% Bi, 58.5 at% Te; bulk (line scan): 41.3 at% Bi, 58.7 at% Te

regime, the anodic peak at +0.48 V increased, as shown in Fig. 2. An accumulation in the limiting current area of the bismuth deposition formed an increased stripping peak current at +0.48 V. However, the peak area between +0.1 V and +0.3 V (Fig. 3) increased, and additional steps were observed. We conclude that, between 0.1 V and 0.3 V, Bi is preferentially oxidized, while at 0.48 V, Te is oxidized.

**Fig. 12** X-ray pattern of  $\text{Bi}_2\text{Te}_3$  powder, electrodeposited on a Ni foil substrate: **(a)**  $\text{Bi}_2\text{Te}_3$  sample deposited on Ni, prepared as a rough milled powder; **(b)**  $\text{Bi}_2\text{Te}_3$  standard (US National Bureau of Standards)



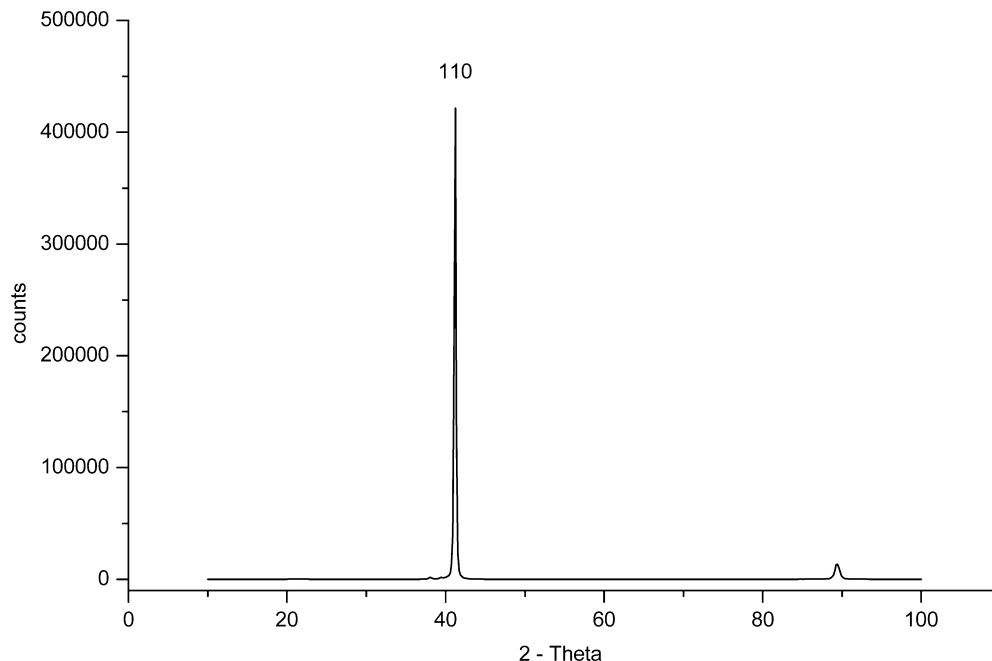
Cyclic voltammograms of the optimized electrolytes (Fig. 4) showed a cathodic deposition peak with  $|E_P - E_{P/2}|$  values of 17–24 mV and one corresponding stripping peak, assigned to the dissolution of one homogeneous bismuth telluride phase. The influence of the stirring rate on the thickness of the diffusion layer was investigated with the help of a rotating disc electrode. The cathodic limiting current density was twice as high at 300 rpm as in the unstirred solution. The currents increased up to 2000 rpm and then became constant. At higher rotation rates the deposition became kinetically controlled. Voltammetric curves for different temperatures are shown in Fig. 5. The shape of the dissolution peak changed with increasing temperature, indicating the influence of heat

on the formation of a homogeneous bismuth telluride phase.

The curve obtained at 313 K shows a large symmetric stripping peak without any shoulder waves. The dissolution peaks of the layers which were deposited at temperatures as high as 333 K disappeared, so we assume that no well-crystallized product could be obtained under these circumstances.

Figure 6 shows the dependence of the tellurium content of the alloy layer on the concentration/mole ratio ( $C_{\text{Bi}}/C_{\text{Te}}$ ) in the electrolyte. If the bismuth/tellurium ratio in the electrolyte was within the limits between 3:3 and 4:3, the layers deposited on Ni foils showed almost identical compositions of 58.5 at% Te.

**Fig. 13** X-ray pattern of  $\text{Bi}_2\text{Te}_3$  powder, electrodeposited on a Ni foil substrate; layer thickness 10  $\mu\text{m}$ , 38.5 at% Bi, 61.5 at% Te; lattice: rhombohedral hexagonal ( $R\bar{3}m$ ) [9]; strong (110) preferred orientation



Finely crystalline and dense precipitates were obtained (Fig. 7). With mole ratios of 2:1 or 1:2, distinctly lower or higher tellurium contents were observed in the layers. The surface of a Bi-Te layer deposited from an electrolyte with a mole ratio Bi:Te=2:1, i.e. a layer rich in bismuth, also favourably showed a fine structure. However, from electrolytes with a mole ratio Bi:Te = 1:2, only coarse crystalline and non-adhesive precipitates were obtained (Fig. 8).

The dependence of the composition of the alloy layers on the current density applied at a constant electrolyte composition of Bi:Te = 1:0.8 is presented in Fig. 9. With current densities lower than 2  $\text{mA}/\text{cm}^2$ , tellurium-rich alloy layers are precipitated. In the 4–7  $\text{mA}/\text{cm}^2$  area, a nearly constant composition of 59 at% Te is obtained. Over 8  $\text{mA}/\text{cm}^2$ , bismuth-rich layers are deposited. With a constant bath composition, the composition of the Bi-Te layers could be controlled via the cathodic current density.

In order to improve the quality of the precipitated layers, several wetting agents and brighteners were added to the electrolytes. The addition of paper-glue made by the Barock company (Dresden) led to the precipitation of bright, adhesive layers. However, the addition caused a rise in the bismuth content of the precipitated layer, which so far could not be compensated by variation of other parameters.

To control the distribution of both components, EDX maps were prepared. For this purpose, the surface in an area of  $18 \times 18 \mu\text{m}^2$  was scanned. In Fig. 10a and Fig. 10b the intensities obtained for bismuth and tellurium are displayed, differentiated by shading. Figure 10c shows the corresponding SEM view of the surface. The homogenous images prove a uniform distribution of bismuth and tellurium. Over the surface, this means a constant composition of the film.

A cross-section of a  $\text{Bi}_2\text{Te}_3$  layer on Ni is shown in Fig. 11a. The layers can be described as a field-oriented texture type (FT), as classified in accordance with Fisher [13]. The line scan (Fig. 11b) proves the constant composition across the layer. X-ray diffraction analysis (Fig. 12 and Fig. 13) shows that the layers grow in the direction of the [110] orientation. The  $c$ -axis of the bismuth telluride hexagonal elementary cell is located parallel to the layer plane [9].

Electrochemical impedance spectroscopy was used to measure  $1/C^2$  versus  $E$  (Mott-Schottky) plots (details to be published). Together with the Hall-effect measurements, it was shown that the deposit was a semiconductor.

For each sample the Hall resistivity  $\rho_H$  was measured as a function of the applied magnetic field  $B$  up to 13 T.

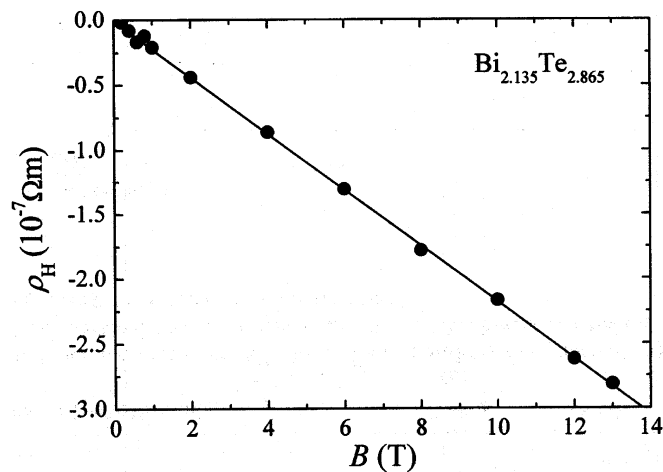


**Fig. 14** Hall resistivity  $\rho_H$  vs. applied field  $B$  at 300 K for  $\text{Bi}_{2+x}\text{Te}_{3-x}$  with  $x=0.135$ . The straight line is a best linear fit to the data



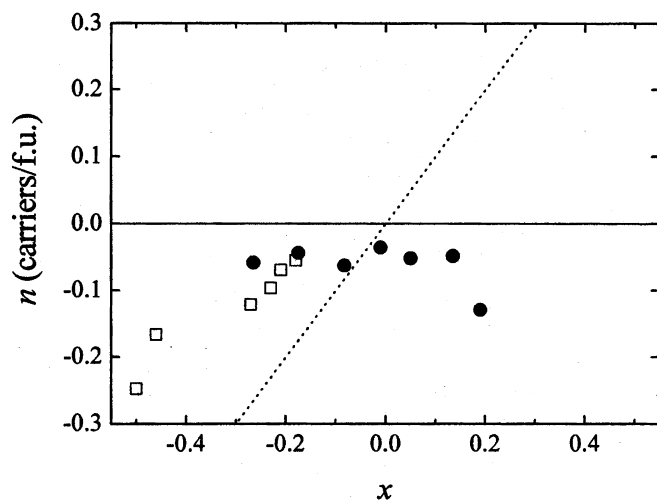


**Fig. 15** Charge carrier concentration  $n$ , as determined from Hall-effect measurements, as a function of  $x$ , the nominal Bi excess in  $\text{Bi}_{2+x}\text{Te}_{3-x}$ . The filled data points are from this work; the open data points are from [3]. The dotted line shows the theoretical expectations

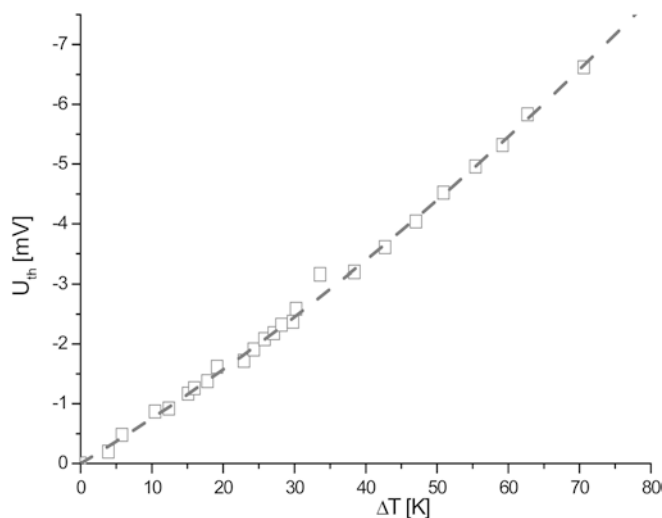


**Fig. 16** Thermo-e.m.f. of bismuth telluride layer (60 at% Te; EDX) measured against Cu strip

A typical curve is shown in Fig. 14. For all samples,  $\rho_{\text{H}}$  is linear with  $B$ . Thus, the Hall constant  $R_{\text{H}} = \rho_{\text{H}}/B$  is field independent. This simple behaviour suggests the interpretation of the Hall coefficient in terms of a simple one-band model, where  $R_{\text{H}} = 1/ne$  ( $n$  is the charge carrier concentration (including sign) and  $e$  the absolute value of the electronic charge). Figure 15 shows the results for all investigated samples together with data from the literature [6]. The charge carrier concentration  $n$  is negative for all investigated samples, i.e. the electrical conduction is of the n-type even in samples with an excess of Bi. It must be pointed out that from the nitric acid electrolyte and the deposition conditions described above, only n-type  $\text{Bi}_2\text{Te}_3$  was obtained.

The electroplating of bismuth telluride onto flexible substrates was performed and transferred to thermogenerator preparation. The thermoelectric properties of the electroplated bismuth telluride were investigated with a measuring set-up without the need for expensive patterning of the couple's strips or complete generators. The electroplated n- $\text{Bi}_2\text{Te}_3$  strips yielded a much higher thermo-e.m.f. compared to Bi (Fig. 16).

## Conclusions

The investigations showed that stoichiometric bismuth telluride could be electrodeposited onto nickel substrates from a nitric acid electrolyte containing  $8.2 \times 10^{-3}$  M bismuth and  $10.3 \times 10^{-3}$  M tellurium. Electrolytes with a Bi:Te molar ratio of 3:3–4:3 could be used. Current densities of 2–5 mA/cm<sup>2</sup> were applied. The alloy deposition occurred under stirring. Soluble anodes were used. The bismuth tellurides were of such a quality that they could be deposited on microelectronic devices. This opens the way to use this process for manufacturing thermoelectric microdevices. X-ray measurements and DTA investigations showed that the coatings could be identified as bismuth telluride ( $\gamma$ -phase). Only n-type semiconductors were deposited under the experimental conditions, verified by the Hall measurements and by electrochemical impedance spectroscopy. To deposit p-type  $\text{Bi}_2\text{Te}_3$ , a new electrolyte must be developed.

**Acknowledgements** This study was supported by the BMWi (Bundesministerium für Wirtschaft) and the AiF (Arbeitsgemeinschaft industrieller Forschungsvereinigungen "Otto von Guericke" e.V.), research no. 12118 BR. The authors are grateful to Dr. B. Hahne (Institute of Chemical Technology and Polymer Chemistry of the Martin-Luther-University Halle, Germany) and Dr. O. Rademacher (Institut of Inorganic Chemistry of the Technical University Dresden, Germany) for performing the X-ray diffraction measurements.

## References

1. Plötner M (1998) Thermobatterie mit galvanisch abgeschiedenen Schenkeln. Abschlussbericht, TU Dresden
2. Qu W, Plötner M, Fischer W-J (2001) J Micromech Microeng 11:146
3. Okamoto H, Tanner LE (1986) In: Massalski TB (ed) Bi-Te (bismuth-tellurium) binary alloy phase diagrams. American Society for Metals, Metals Park, Ohio
4. Gmelin (1964) Handbuch der anorganischen Chemie. Bismut Ergänzungsband. Verlag Chemie, Weinheim, p 800
5. Magri P, Boulanger C (1995) AIP Conf Proc 316:277
6. Magri P, Boulanger C, Lecuire JM (1996) J Mater Chem 6:773
7. Fleurial J-P, Herman J-A, Snyder G-J, Ryan MA, Borschchewsky A, Huang C-K (2000) Mater Res Soc Symp 626:Z11.3.1
8. Montiel-Santillán T, Solorza O, Sánchez H (2002) J Solid State Electrochem 6:433
9. Cheaoui H, Bessieres J, Modaressi A, Heizmann JJ (2000) J Appl Electrochem 30:419
10. Lenher V, Wakefield HF (1923) J Am Chem Soc 45:1423

11. Lang R, Faude E (1937) *Z Anal Chem* 108:260
12. Maclachlan JM, Kruesi WH, Fray DJ (1992) *J Mater Sci* 00:000
13. Fischer H (1954) *Elektrolytische Abscheidung und Elektrokristallisation von Metallen*. Springer, Berlin Göttingen Heidelberg, p 485
14. Budevski E, Staikov G, Lorenz WJ (1996) *Electrochemical phase formation and growth*. VCH, Weinheim, p 71
15. Mamantov G, Manning DL, Dale JM (1965) *J Electroanal Chem* 9:253
16. Berzins T, Delahay P (1953) *J Am Chem Soc* 75:555